Article no. 49

THE CIVIL ENGINEERING JOURNAL 4-2018

3D DYNAMIC TIME-HISTORY RESPONSE ANALYSIS OF AN ISLAND PLATFORM METRO STATION IN LOESS AREA

Wang Ke[1,2], Siyue He[2], Guanglong Zhang[3]*

1. *China Railway First Survey and Design Institute Group CoLtd., Xi'an 710043, China*
2. *School of Highway, Chang'an University, Xi'an 710064, China; hesiyue@chd.edu.cn, 408423231@qq.com*
3. *Shandong Academy of Building Research, Ji'nan 250031, China*

ABSTRACT

Through the years, the seismic resistance of underground structures has attracted more and more attention, and dynamic characteristics of metro station is one of the most important issues. In this article, the 3D numerical model of Zhang Wangqu metro station along Metro Line 5 in Xi'an is established to study on seismic dynamic response of roof, floor, columns and beams in the island platform metro station. Compared with the earthquake damage of Dakai metro station in the Kobe M7.2 Earthquake and the shaking table test of metro station in loess area, results reveal that horizontal acceleration can reflect seismic wave characteristics under the horizontal seismic wave; the maximum relative displacement of roof and floor, the maximum axle force and shear force at transfer node are bigger than the standard section and reduce with the increase of buried depth; the maximum axle force and shear force of columns increases from top to bottom. The island platform metro station should focus on the structural settings of transfer node, and the columns and beams here must select materials with greater strength.

KEYWORDS

Dynamic characteristics, Xi'an Metro, 3D numerical model, Island platform metro station, Transfer node, Dynamic seismic analysis

INTRODUCTION

With the rapid development of China's economy, the ground transportation system can no longer meet the demand of passenger transportation in urban traffic, and the development of Urban Rail Transit System with underground railway as the backbone is the main way to solve the traffic problems in big cities. Due to restrained effect of soil layer, compared with the ground structures, seismic performance of the underground structures is stronger, and its seismic capacity strengthens with the increase of buried depth. Due to the short history of underground constructions, the dynamic response and seismic research of underground structures is not enough. While the Kobe

M7.2 Earthquake of Japan in 1995, the Chi Chi M7.6 Earthquake of Taiwan in 1999, the Wenchuan M8 Earthquake of Wenchuan in 2008, the metro stations were seriously damaged, the ground sank, the columns and beams cracked and collapsed; the study of seismic response and seismic resistance of underground structures is gradually improving. In recent decades, the research on metro station seismic resistance has focused on theoretical research, shaking table test and numerical simulation. For theoretical research, Zhuang [1], Liu [2], and Wang et al. [3] utilized the seismic response displacement method of soil-structure interaction and nonlinear analysis of equivalent inertial force method to correct the calculation theory of FEM and improve the seismic response system of metro station. For shaking table test, Yang [4], Bian [5], Jing [6], Chen [7], Zhuang [8], Chen [9], and Quan et al. [10, 11] carried out shaking table test of metro station on liquefiable foundation and studied the seismic response of three-arch and multi-storey metro station in loess region. For numerical simulation, Parra-Montesinos [12], Du [13], and Liu et al. [14] combined the destruction of Dakai metro station by Kobe M7.2 Earthquake of Japan in 1995 and used FEM to establish numerical model, analysed the mechanism of earthquake damage at different location of the metro station. Liu [15], and Bao et al. [16] used FEM to establish numerical model for metro station in the liquefiable soil layer, and studied the seismic response of metro station under horizontal and vertical seismic waves. Wang [17], Zhuang [18], and Li et al. [19] used FEM to establish numerical model for metro station in soft soil, and analysed the seismic response and failure mechanism of metro station with different depths, layers and structures. For comprehensive analysis, Chen [20, 21] and Moghadam et al. [22] carried out shaking table test and used FEM to establish numerical model for test, compared the results of shaking table test and numerical simulation, and studied the seismic response of metro station deeply. These studies are based on structural dynamics, mainly study the seismic responses of the columns and some structures of metro station, and do not analyse the difference between the seismic response of metro station with different structures, so there is no systematic and comprehensive analysis of the earthquake response of the island platform metro station.

China is between the Eurasian seismic belt and the Pacific seismic belt, the earthquake is frequent, and loess is widely distributed. Loess has the special structure of columnar joints, large pores, weak cementation and special sensitivity to water, which makes the earthquake damage in loess area very serious. Xi'an Metro is the first subway project to build in the loess area, and there have been three earthquakes above magnitude 7 and eleven earthquakes above magnitude 6; the island platform metro station has the advantages of economical use, large capacity, etc., and has been widely adopted, so the seismic response analysis of island platform metro station in Xi'an is of great significance.

BACKGROUND

Zhang Wangqu metro station is the ninth station of the Metro Line 5 in Xi'an and located on the east intersection of the Kunming Road and the Feng Jing Avenue [23, 24]. The metro station is two layers excavated island platform station and total floorage is 17,386 m², the main building area is 12,414 m², and the ancillary floor area is 4,972 m². The metro station is provided with four entrances,

two groups of wind pavilions, and a safe entrance. The total length is 245.25m, overall width of standard section is 22.7 m, the depth of metro station is 14.34～16.121 m, and thickness of covering soil is 2～4 m, the main design parameters are shown in Table 1. The reinforced concrete frame structure with double columns and three-span is used in the metro station, the standard section is divided into two layers, as shown in Figure 1(a), and the transfer joint is divided into three layers, as shown in Figure 1(b).

According to geological investigation, landforms along the metro station are divided into the Weihe bench land, the Feng He River bed, and the primary alluvial terrace and residual two stage alluvial terrace. The geological exploration depth is within 50.0 m, and the stratum is mainly quaternary accumulation, new artificial fill (Q^{4ml}), loess, medium sand and silty clay (Q^{4al+pl}), and silty clay (Q^{3pl}). The floor of the metro station is located in the medium sand layer. The thickness of the surface filling layer is about 0.40～1.50 m, the main ingredients are crushed brick and concrete, mainly for the construction waste. The thickness of plain filling layer 0.40～12.80 m, the main components is the silty clay, containing a small amount of ash and slag brick, sand, uneven soil, mainly for road backfill of the Keyuan Road and site backfill of the Qili town in Xi'an.

Tab. 1 - Design parameters of the Zhang Wangqu station

Item	Zhang Wangqu station
Metro station structure	Island platform metro station (Two layers and L type transfer)
Construction method	Open Cut Method
Total length	245.25 m
Total width	22.7 m
Thickness of soil	2～4 m
Depth of metro station	Depth of floor 1 5m（Local depth 22 m）
Main column distance	9.75 m

DOI 10.14311/CEJ.2018.04.0049

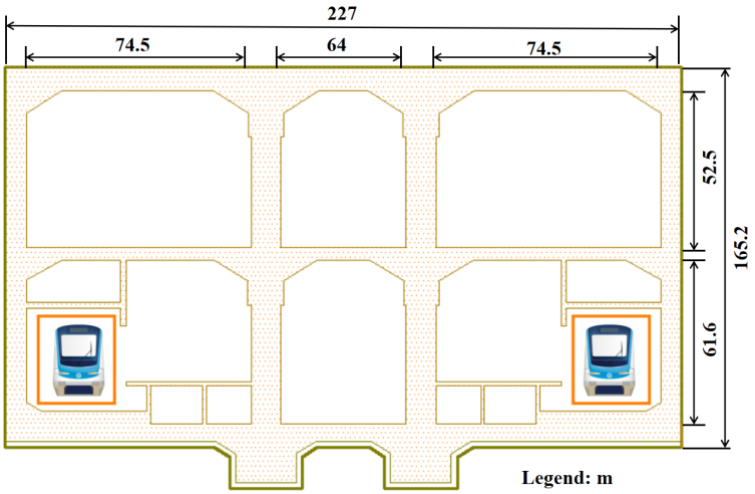

(a) Cross section of standard structure

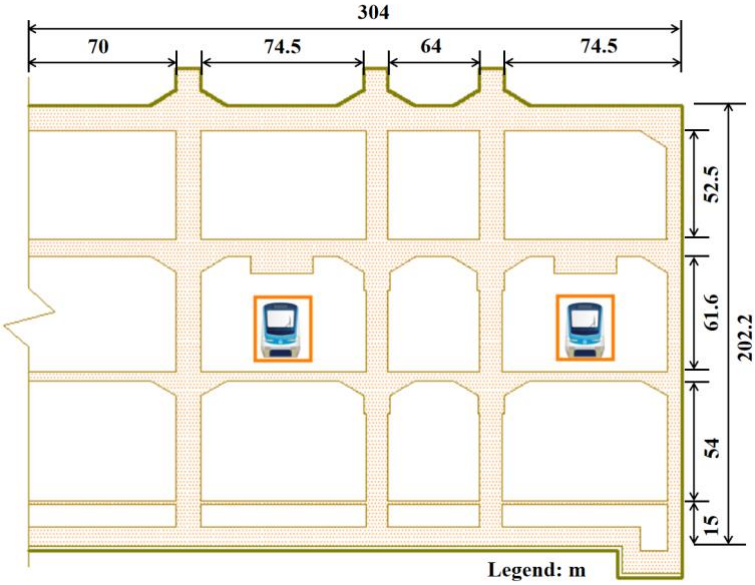

(b) Cross section of transfer joint

Fig. 1 - Section of subway station

NUMERICAL MODEL

Based on the Midas-GTS software, numerical analysis is carried out, the rock mass in the numerical model is simulated with solid element, and the constitutive model uses the Mohr-Coulomb to consider nonlinear deformation; the columns and beams are simulated by beam element, the exterior wall and floor are simulated with plate elements, and the constitutive model uses the linear elastic model. The concrete strength grade of roof, floor, the exterior wall is C30; the concrete strength grade of columns and beams is C45; the grade of steel is HRB400. In the

horizontal direction, the distance between the artificial boundary and the underground structure of the numerical model is 3 times the effective width of the metro station; in the vertical direction, the distance between artificial boundary and the numerical model is 3 times the effective height of the metro station. The length of the numerical model is 586 m, width is 253 m, height is 47 m, the soil layers are divided into six layers, from the top to bottom are filling soil, loess soil, silty clay 1, medium sand 1, silty clay 2, and medium sand 2. The unit size is between 1/10 and 1/8 of the maximum wavelength of the input wave [25], the whole numerical model is divided into 133,655 nodes and 123,405 units. The material parameters of the soil layers are shown in Table 2, and the material parameters of the metro station structure are shown in Table 3, the finite element network of the whole system is shown in Figure 2, the detail structure of metro station and measuring points layout are shown in Figure 3(a), the beams, columns and measuring points layout of the metro station are shown in Figure 3(b).

Tab.2 - The material parameters of the soil layers [26]

Soil type	Depth /m	Density/ g•cm^{-3}	Shear wave velocity/m•s^{-1}	Longitudinal wave velocity/m•s^{-1}	Dynamic modulus of elasticity/MPa	Dynamic shear modulus/MPa	Poisson's ratio
Filling soil	3.5	1.9	210.3	378.1	293.8	101.3	0.33
Loess soil	4	2	107.5	187.9	162.4	56	0.26
Silty clay 1	4.3	1.9	405.8	763.2	568.1	195.9	0.4
Medium sand 1	8.9	1.9	210.4	374.8	290.9	100.3	0.32
Silty clay 2	6.3	1.9	619.6	1176.3	870.7	290.3	0.3
Medium sand 2	20	1.9	312.5	580.4	416.1	148.6	0.32

Tab. 3 - Material parameters of metro station

Component	Unit weitht/kN•m^{-3}	Modulus of elasticity/GPa	Poisson's ratio	Size/m
Exterior wall	24	31	0.2	a
Roof	24	31	0.2	b
Beams	24	31	0.2	0.6*0.6
Columns	24	2.4	0.2	0.7*1.2
First floor	24	31	0.2	c
Second floor	24	31	0.2	d
Third floor	24	31	0.2	e

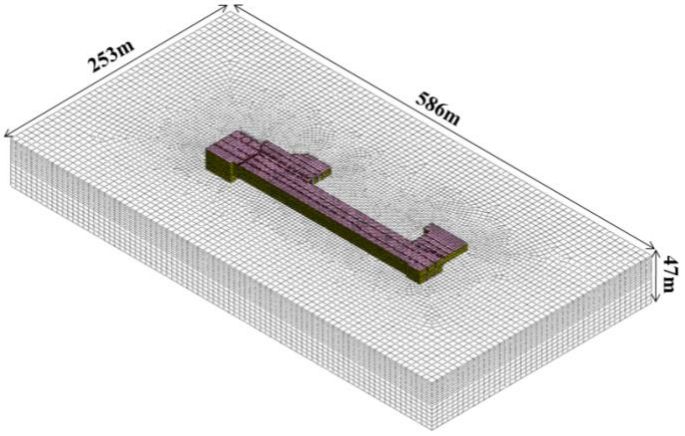

Fig. 2 - The finite element network of the whole system

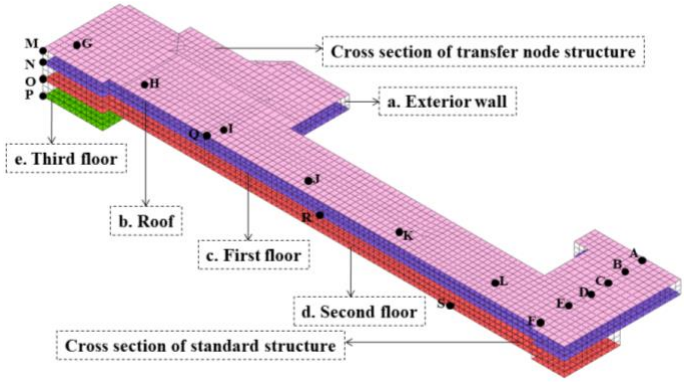

(a) Measuring points layout of metro station

Fig.3 - Detail structure and measuring points layout and beams and columns of metro station

DOI 10.14311/CEJ.2018.04.0049

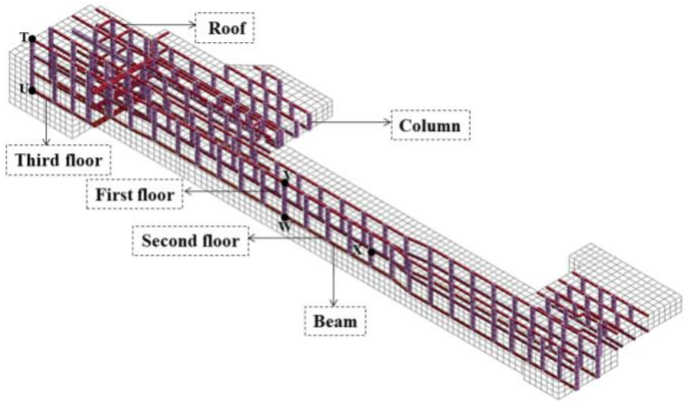

(b) Beams and columns of metro station

Fig.3 - Detail structure and measuring points layout and beams and columns of metro station

BOUNDARY CONDITIONS AND DAMPING SETTINGS

For the limited range of computing areas, the wave energy will be reflected on the artificially boundary under the action of seismic waves, causing the wave to oscillate, resulting in simulated distortion [27-30]. To solve the problem of wave reflection on the boundary of numerical model, the boundary conditions adopt the viscoelastic absorbing boundary proposed by Deeks et al. [25]. The viscoelastic boundary can not only simulate the radiation damping of the foundation, but also simulate the elastic recovery performance of the earth medium, and it has good low frequency stability, the vertical ground response coefficient and horizontal ground reaction coefficient are as Formula 1 and Formula 2, the reaction coefficient of foundation is 1 [31-32]. In eigenvalue analysis, the first ten order values are taken, among them, the first and second order of mass participation coefficient is highest, the characteristic cycles are 1.059 s and 0.999 s; Rayleigh damping is used in the time-history analysis of the numerical model, the fixed bottom condition is selected, and its damping are calculated as Formula 3 and Formula 4.

$$k_v = k_{v0} \cdot (\frac{B_v}{30})^{-\frac{3}{4}} \tag{1}$$

$$k_h = k_{h0} \cdot (\frac{B_h}{30})^{-\frac{3}{4}} \tag{2}$$

Among them：

$$k_{v0} = \frac{1}{30} \cdot \alpha \cdot E_0 = k_{h0}, B_v = \sqrt{A_v}, B_h = \sqrt{A_h}$$

A_v and A_h are the cross sectional area of vertical and horizontal element, respectively. E_0 is the modulus of elasticity of the soil, α is 1.0.

For P waves:

$$C_p = \rho \cdot A \cdot \sqrt{\frac{\lambda + 2G}{\rho}} = W \cdot A \cdot \sqrt{\frac{\lambda + 2G}{W \cdot 9.81}} = c_p \cdot A \tag{3}$$

For S waves:

$$C_s = \rho \cdot A \cdot \sqrt{\frac{G}{\rho}} = W \cdot A \cdot \sqrt{\frac{G}{W \cdot 9.81}} = c_s \cdot A \tag{4}$$

Among them：

$$G = \frac{E}{2(1+\nu)}, \lambda = \frac{\nu E}{(1+\nu)(1-2\nu)}$$

E is the modulus of elasticity of the soil, *v* is the Poisson's ratio, *A* is the boundary area. That is the area of the boundary on both sides of the model.

SEISMIC WAVE

Xi'an is located at the southwest end of the Fen Wei fault depression, belonging to the middle and strong seismic belt. Since the second century BC, there have been 128 earthquakes with magnitude greater than 4, including 25 earthquakes over 5. Zhang Wangqu metro station belongs to the general area of earthquake fortification, the site category is class II field, for non collapsibility ground, collapsibility grade is I, the maximum thickness of the collapsibility of 4.2vm; there is no seismic liquefaction, and there is no bad geological phenomenon like ground fissure, landslide, collapse, etc. In view of seismic safety evaluation report of the Xi'an metro line 5, we simulate the seismic fortification intensity of 8 degree, the peak ground acceleration (PGA) Ag is 0.20 g, the characteristic period is partitioned into II areas, spectrum cycle partition value Tg is 0.40 s, and time-history seismic waveform in the numerical model is shown in Figure 4. The attenuation coefficient of seismic wave is 0.85 at the X boundary, the damping ratio of all vibration modes is 0.05, the loading time is 20 s, the analysis time step is 0.4 s, the output time step is 1, and the output is 50 steps.

DOI 10.14311/CEJ.2018.04.0049

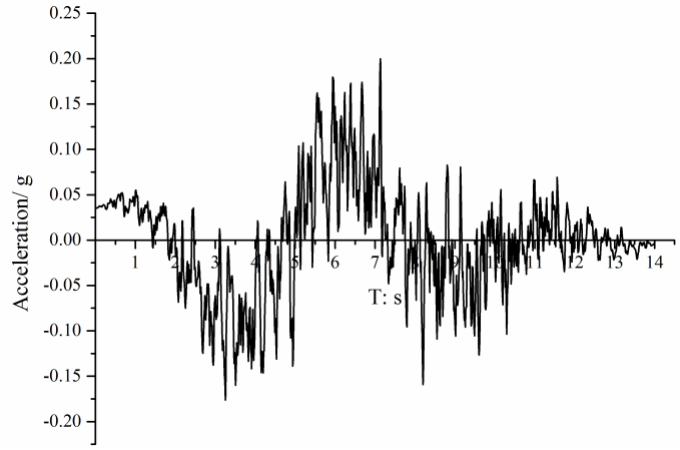

Fig. 4 - Seismic waveform

RESULTS ANALYSIS

Displacement analysis

Absolute displacement analysis

The displacement measuring points A-E along the Y axis are arranged, and the displacement measuring points G-L along the X axis are arranged, and the displacement measuring points M-P along the Z axis are arranged shown in Figure 3. The vertical displacement of the metro station is positive value, the metro station floats; along the X and Y directions, the maximum vertical displacement shows a depression, the maximum vertical displacement of measuring points C and J is the minimum; along the Z direction, the maximum vertical displacement of the middle is basically unchanged; the maximum vertical displacement in each direction shows that the middle is smaller. The horizontal direction of seismic wave has no effect on the Z axis direction of the maximum vertical displacement. The displacement measuring points M, Q, R and S of roof and floor are shown in Figure 5(a), the vertical displacement time-history curve is shown in Figure 5(b). The vertical displacement of the roof is measuring point M and Q, and the vertical displacement of the first floor is measuring point R, and the vertical displacement of the second floor is the measuring point S. Before 14s, the vertical displacement curve of different plates is similar, and reaches the peak at the same time, with the increase of buried depth, the vertical displacement decreases, but after 14s, the seismic wave unloads, the metro station moves slightly under the action of inertia force, but it is basically in stable state.

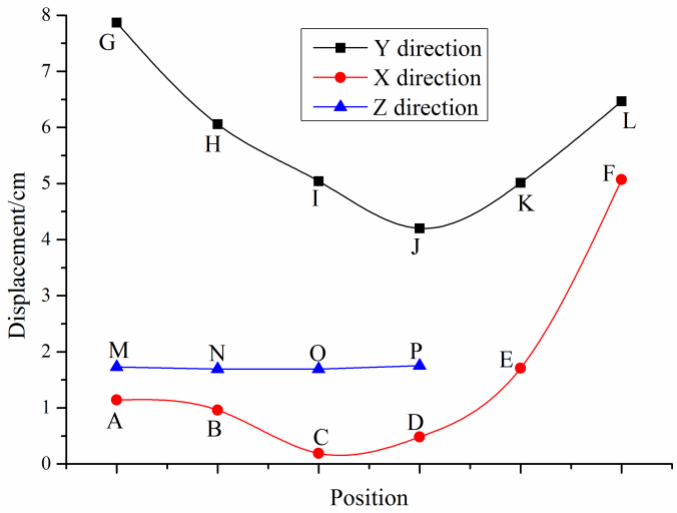

(a) Maximum vertical displacement

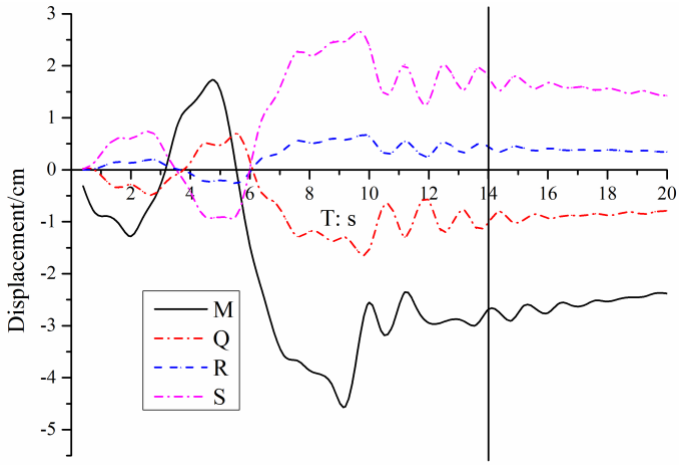

(b) Time-history of maximum vertical displacement

Fig. 5 - Maximum vertical displacement and time-history of maximum vertical displacement

Relative displacement analysis

The relative displacement measuring points M, R, S, P of the roof and floor are shown in Figure 3, the measuring point M is located in the roof, R is located in the first floor, measuring point S is located in the second floor, and measuring point S is located in the third floor. The horizontal relative displacement time-history curve is shown in Figure 6, the relative horizontal displacement curve of measuring points M, R, S, P is similar to seismic wave fluctuation. Before 14 s, the relative horizontal displacement of the second floor is the maximum, the relative horizontal displacement of the third floor is the minimum. The maximum horizontal relative displacement of crest is smaller, the maximum horizontal relative displacement of trough is larger. After 14 s, the maximum horizontal

relative displacement is almost constant, and the maximum relative displacement between of different floor is a fixed value.

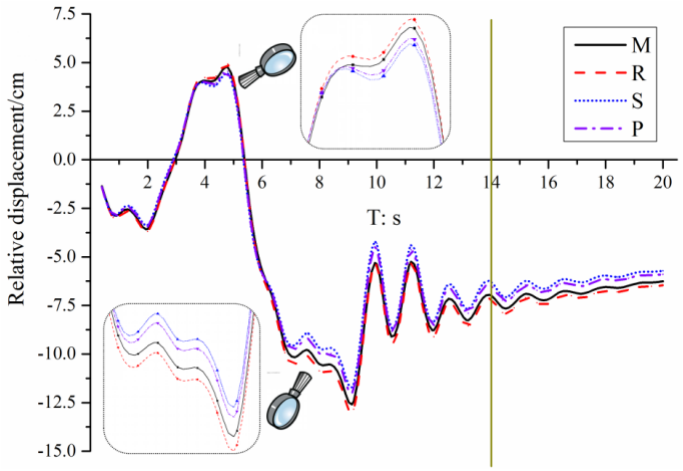

Fig. 6 - Maximum relative horizontal displacement of measuring points

Acceleration analysis

Acceleration analysis of sidewall

The acceleration measuring points M and S of sidewall are shown in Figure 3. The maximum horizontal acceleration in the standard section is the maximum, the maximum horizontal acceleration in the transfer node is the minimum. The maximum vertical acceleration at the transfer node is large, especially in the corner, the vertical acceleration reaches the maximum value; the maximum vertical acceleration in the standard section is small. The horizontal acceleration time-history of the measured points M and S are shown in Figure 7(a), and the vertical acceleration time-history of the measured points M and S are shown in Figure 7(b). Under the action of horizontal seismic wave, the horizontal acceleration time-history curves of the measuring points M and S are almost identical and can reflect the seismic waveform, the role of the stratum is equivalent to the spring, and the seismic wave is reduced after loading on the metro station; the vertical acceleration of measuring points M and S is distorted and cannot reflect the seismic waveform. With the increasing buried depth of metro station, the horizontal and vertical acceleration decreases.

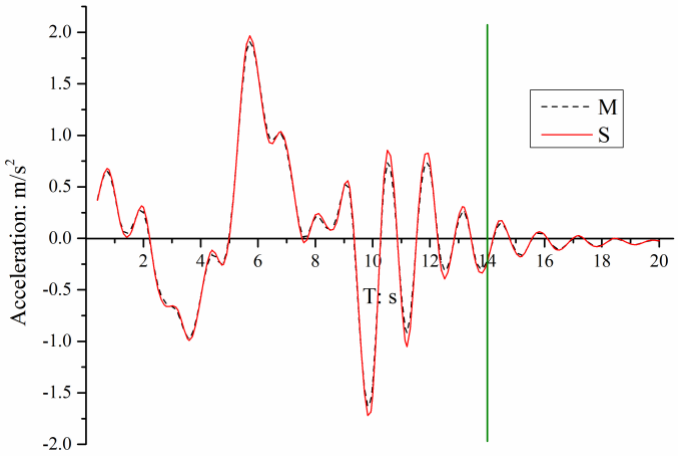

(a) Maximum horizontal acceleration

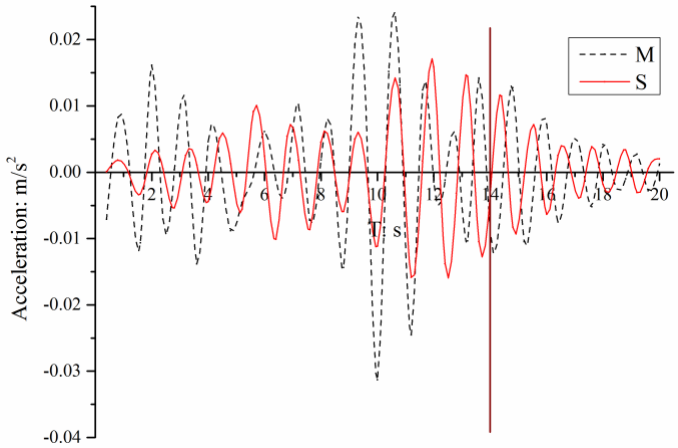

(b) Maximum vertical acceleration

Fig. 7 - Time-history of maximum horizontal and vertical acceleration of measuring points

Acceleration analysis of roof and floor

The acceleration measuring points M, R, S and P of roof and floor are shown in Figure 3. The horizontal acceleration of standard section is large, the horizontal acceleration of transfer node is small. The vertical acceleration of transfer node is big, the vertical acceleration of standard section is small. The horizontal acceleration time-history curve of M, R, S and P are shown in Figure 8(a), and the vertical acceleration time-history curve is shown in Figure 8(b). Before 14s, the horizontal acceleration curve of floor and roof is similar and both can reflect seismic waveform, wherein the horizontal acceleration peak value of the first floor is the maximum, the horizontal acceleration peak value of the fourth floor is the minimum, but the difference between the two plates is small. With the increase of the buried depth, the horizontal acceleration at the floor and roof decreases. The vertical acceleration time-history curves of the floor and roof are quite different and cannot reflect the

seismic waveform. After 14s, the vertical acceleration time-history still fluctuates greatly, which indicates that the inertia force has a great influence on the vertical direction of the metro station.

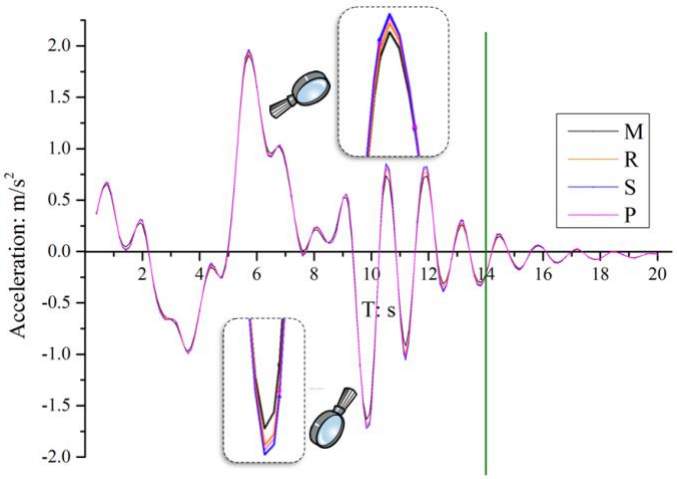

(a) Maximum horizontal acceleration

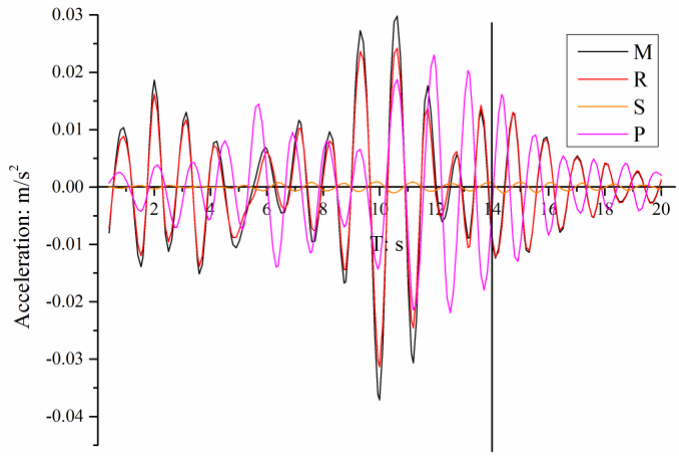

(b) Maximum vertical acceleration

Fig. 8 - Time-history of maximum horizontal and vertical acceleration of measuring points

Internal force analysis

Internal force analysis of columns

There are 123 columns in the metro station. The measuring points T, U, V, W at the top and the bottom of the columns are shown in Figure 3, and the axial force time-history of measuring points is in Figure 9(a). Before 14 s, the axle force at the top and the bottom of the columns in transfer node is large, the fluctuation range is large, and the maximum tension is 198 kN, the maximum pressure of 387kN, while the axle force at the top and the bottom of the columns in transfer node is small, the maximum tensile force is 8kN, the maximum pressure of 42 kN. After 14 s, the seismic wave

unloads, the axle force of the columns decreases and gradually tends to a steady state. The shear force time-history of measuring points is in Figure 9(b). Before 14s, the shear force at the top and the bottom of the columns in transfer node is large, and the fluctuation range is large, while the axle force at the top and the bottom of the columns in transfer node is small, and the volatility is not obvious. The top and bottom of the columns is under the interaction of axial force and shear force in different direction, the "shear compression effect" is more obvious than "shear pull effect", and the two effects exist simultaneously, resulting in the destruction of columns.

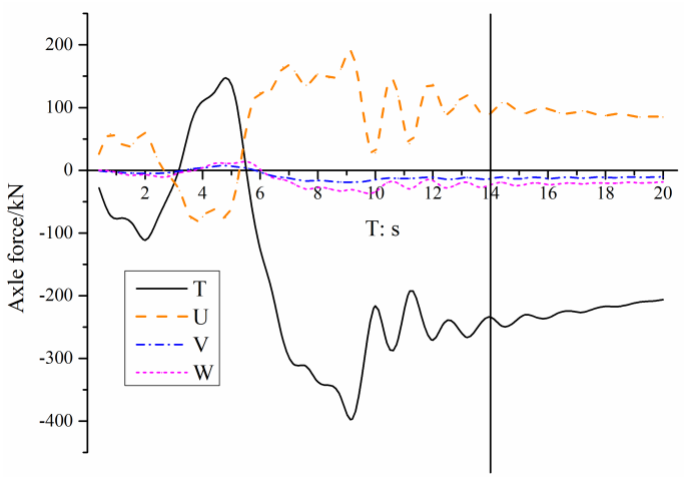

(a) Axle force

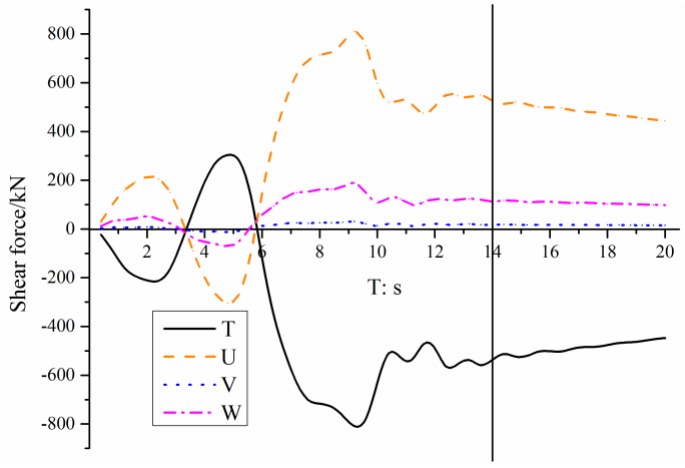

(b) Shear force

Fig. 9 - Time-history of axle force and shear force of measuring points

Internal force analysis of beams

The metro station is divided into four layers of beams. The measuring points T, U, W, X of different beams is shown in Figure 3, the axial force time-history of beams is as shown in Figure 10(a). The axial force of measuring point T is the maximum, the maximum tensile force is 1679kN, the maximum pressure is 605kN; the axial force of measuring point X is the minimum, the maximum tensile force is 236kN, the maximum pressure is 498 kN, the axial force of measuring points U and W is between the measuring point X and T. With the increase of buried depth, the axial force of beams reduces, and axial force difference between different layers of the beams increases. Before 14s, the axial force fluctuation of beams is large, the range between crest and trough is also large, on the same floor, the beam may be partly pulled and partly compressed. After 14s, the seismic wave unloads, under the action of inertia, the axial force of beams decreases and gradually tends to be stable. The shear force time-history of measuring points T, U, W, X is shown in Figure 10(b), the shear force of measuring point X is the maximum, the maximum shear force is 78 kN, the minimum shear force is 32 kN; the shear force of measuring points U and W is the minimum, the maximum shear force is 11 kN, the minimum shear force is 4 kN; so shear force at the transfer node beam is small, while the shear force of standard section is small. Before 14 s, the shear force fluctuation of beams is large, the range between crest and trough is also large. The shear force of beams is less than 100 kN, therefore, the beam shear has little effect on the beam strength; the maximum axial force of beams is 1679kN, therefore, the damage of the beams may be caused by the excessive tension.

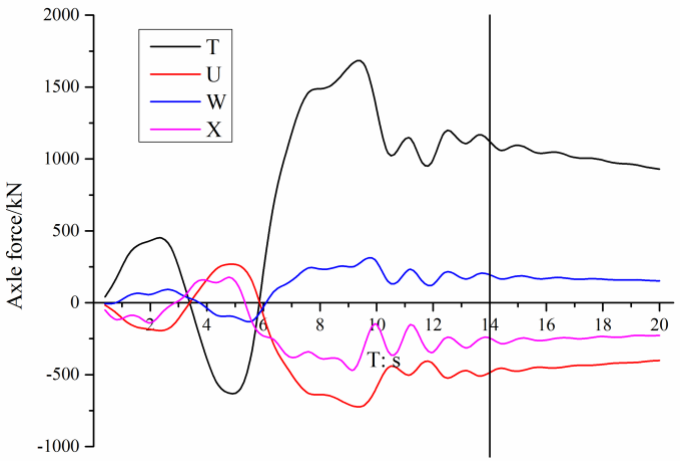

(a) Axle force

Fig. 10 - Time-history of axle force and shear force of measuring points

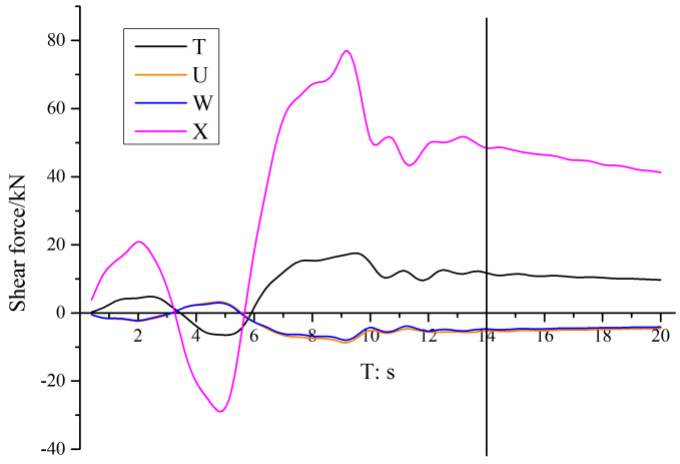

(b) Shear force

Fig. 10 - Time-history of axle force and shear force of measuring points

DISCUSSION

Earthquake damage of metro station

The Mexico earthquake in 1985, the subway tunnel was dislocated. The Loma Prieta earthquake in 1989, the Alameda immersed tube tunnel cracked in the Gulf of San Francisco, where water seepage and floating phenomena occurred. The Wenchuan earthquake in 2008, many tunnels in the Dujiangyan-Wenchuan Expressway near the epicenter were seriously damaged, there are lining cracking, floor heave, steel exposed, lining seepage and so on. The Kobe M7.2 Earthquake of Japan in 1995, the destruction of subway structure is the most serious. In the earthquake, a total of 5 metro stations and 3km tunnel were destroyed to varying degrees, the Dakai metro station suffered the most serious damage [13], as shown in Figure 11(a). The columns broke, the roofs collapsed, and the ground subsidence appeared. The destruction of the metro station is almost impossible to repair, which directly aroused the attention of Japan to the earthquake science and the earthquake resistance of underground structures.

(a) Earthquake Damage of Dakai metro station [13]

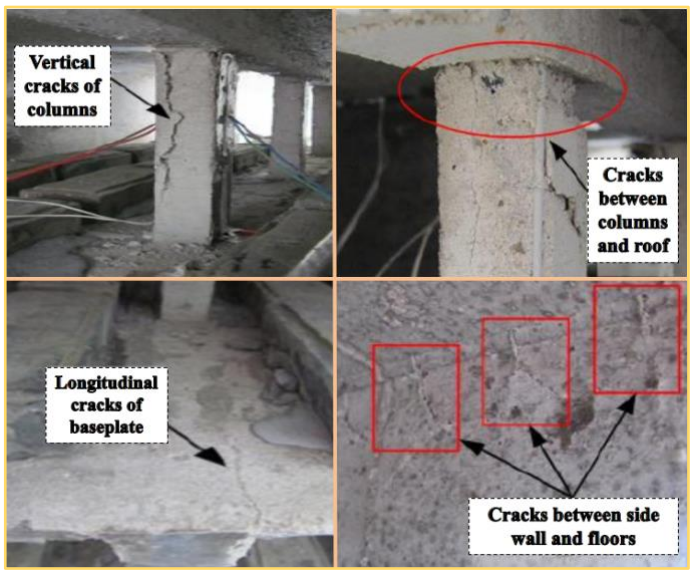

(b) Destruction of metro station in shaking table test [10, 11]

Fig. 11 - Earthquake damage of Dakai metro station and destruction of metro station in shaking table test [10, 11, 13]

Shaking table test of metro station

Matsui Jun et al. [33] carried out the earliest shaking table test of underground structures. In recent years, the shaking table test has been widely used in the study of soil-pile-superstructure interaction. Some scholars have gradually applied the shaking table test to the seismic research of metro station, as shown in Table 4. Based on the analysis of the stratum of Shanghai Metro, Yang et

al. [4] established the shaking table test of double-deck and three-span metro station, and obtained the time-history of acceleration, structural stress, and soil surface deformation of the model; Chen et al. [7, 20, 21] conducted a large shaking table test on liquefiable sand foundation in Nanjing, the reaction law of pore water pressure and acceleration response of the model were analysed; Bian et al. [5] carried out shaking table test of geological conditions in Beijing area, analyzed the time-history of dynamic stress, and studied the acceleration and stress distribution in different positions of the metro station; Cheng et al. [34] conducted the shaking table test of three-layer metro station, obtained the conclusion that failure of multi-layer metro station was controlled by displacement and improving the ductility of the structure was an effective method to improve the seismic performance of the underground structure.

For earthquake resistance of metro station in loess area, Quan et al. [10, 11] took the metro station of Xi'an Metro Line 4 as the prototype structure, and used the loess, granular concrete and galvanized steel wire to carry out shaking table test of the rectangular double-deck and two-span metro station. He found there was serious structural damage in metro station model. The upper columns occurred typical "shear compression failure" and appeared serious vertical cracks. The concrete in the columns peeled off, the longitudinal steel bar exposed, and destruction of the joint between the upper columns and the roof and the connection between the columns and the roof was the most serious. Cracks occurred at the joint between the side wall and the floor, in addition to the connection between the components, the roof, floor and other parts of the side wall had not obvious damage. Under the action of horizontal seismic wave, columns in frame-type metro station bear the vertical pressure and horizontal shear force; and compared with the side wall, floor, the section and integral stiffness of the columns are smaller, thus serious damage. The typical earthquake damage of metro station in loess area is as shown in Figure 11(b). The Zhang Wangqu metro station along Xi’an Metro Line 5 is similar to it.

Tab. - 4 Material parameters of metro station

Scholar	Examination Contents	Model box	Soil and similar materials	Performance of shaking table
Yang Linde [4]	Shaking table test of metro station in soft soil in Shanghai (Double-deck and double-span structure)	Rigid model box	Raw soil, silty clay, particulate concrete, galvanized steel wire	Platform size: 4m*4m Maximum load: 15t
Chen Guoxing [7, 20, 21]	Shaking table test of metro station in liquefied fine sand in Nanjing (Double-deck and double-span structure)	Rigid model box	Raw soil, fine sand, undisturbed soil, galvanized steel wire	Platform size: 6m*6m Maximum load: 80t
Bian Jin [5]	Shaking table test of metro station in sandy silt in Beijing (Double-deck and double-span structure)	Rigid model box	Raw soil, sandy silt, fine grained concrete, barbed wire	Platform size: 12.3m*18.7m Maximum load: 10t
Cheng Xinjun [34]	Shaking table test of metro station in Harbin (Three-deck and three-span structure)	Cascade shear box	Raw soil, fine particle concrete, fine steel wire	Model proportion: 1:30
Quan Dengzhou [10, 11]	Shaking table test of metro station in loess in Xi'an (Double-deck and double-span structure)	Cascade shear box	Raw soil, loess, particle concrete, galvanized steel wire	Platform size: 3.36m*4.86m Maximum load: 25t

CONCLUDING REMARKS

Through the dynamic time-history response analysis of the Zhang Wangqu metro station in the Xi'an Metro Line 5, compared the numerical simulation results with seismic damage of Dakai metro station in Japan and shaking table test of large metro station in loess area, the following conclusions are obtained:

(1) The relative displacement of roof and floor reaches the maximum at transfer node and reduces with the increase of buried depth. If the earthquake intensity is large enough, it is very possible to dislocate at the transfer node in island platform metro station.

(2) Under the horizontal seismic wave, the horizontal acceleration time-history of metro station can reflect seismic wave characteristics, but the vertical acceleration is distorted and cannot reflect the seismic waveform.

(3) The maximum axial force of columns emerges in the corner transfer node, and the axle force of the other columns is small and uniform; the maximum shear force of beams occurs at both

ends of the metro station, and shear force of columns gradually increases from top to bottom, which may be manifested as shear cracking.

(4) With the increase of buried depth, the maximum axial force of different layer beams reduces and becomes more uneven, so the fatigue failure is easy to occur; the maximum shear force is generated at the end of the beams and is larger at the transfer joint than the standard section of the metro station, which may cause cracks.

(5) For island platform metro station, the columns and at the transfer node have bigger internal force than other positions, so the strength of the columns here needs to be increased; the internal force of beams increases with the increase of buried depth, so the beams in the depth requires greater intensity.

COMPETING INTERESTS

The authors declare that there is no conflict of interests regarding the publication of this paper.

ACKNOWLEDGEMENTS

This work is financially supported by the Brainstorm Project on Social Development of Shaanxi Provincial Science and Technology Department (No. 2016SF-412) and theSpecial Fund for Basic Scientific Research of Central Colleges of Chang'an University (No. 310821172004, No. 310821153312, No. 310821165011) and the National Key R&D problem of China (No. 2017YFC0805306). We also acknowledge the editor for the valuable suggestion.

REFERENCES

[1] H. Y. Zhuang, H. Long, G. X Chen, "Analysis of thenonlinear earthquake responses of a large complicated subway underground station", *Journal of Earthquake Engineering and Engineering Vibration*, Vol. 33, no. 2, pp. 192-199, 2013. (in Chinese)

[2] J. B. Liu, W. H. Wang, G Dasgupta, "Pushover analysis of underground structures: Method and application", *Science China Technological Sciences*, Vol. 57, no 2, pp. 423-437, 2014.

[3] G. F. Wang, X. F. Shang, X. F. Ma, X. Y. Xu, "Equivalent Inertial Force Method of Seismic Calculation for Subway Station in Soft Site", *Shock and Vibration*, Vol. 2016, Article ID 4751071, 9p. doi: 10.1155/2016/4751071.

[4] L. D. Yang, Q. Q. Ji, Y. L. Zheng, C. Yang, D. L. Zhang, "Design of a shaking table test box for a subway station structure in soft soil", *Frontiers of Architecture and Civil Engineering in China*, Vol. 1, no 2, pp. 194-197, 2007.

[5] J. Bian, L. J. Tao, W. P. Zhang, B Zhang, "Shaking Table Test on Dynamic Soil Stress of the metro station Structure", *Chinese Journal of Underground Space and Engineering*, Vol. 7, no 4, pp. 687-690, 2011. (in Chinese)

[6] L. P. Jing , X. C. Meng, H. F. Sun, Y. Zou, B. D. Lu, "Shaking table test analysis of three-story subway station", *Journal of Earthquake Engineering and Engineering Vibration*, Vol. 31, no 6, pp. 159-166, 2011.

[7] G. X. Chen, Z. H. Wang, X. Zuo, X. L. Du, H. M. Gao, "Shaking table test on the seismic failure

characteristics of a metro station structure on liquefiable ground", *Earthquake Engineering and Structural Dynamics*, Vol. 42, no 10, pp. 1489-1507, 2013.

[8] H. Y. Zhuang , Z. H. Hu, X. J. Wang, G. X. Chen, "Seismic responses of a large underground structure in liquefied soils by FEM numerical modeling", *Bulletin of Earthquake Engineering*, Vol. 13, no 12, pp. 3645–3668, 2015.

[9] Z. Y. Chen, W. Chen, X. Y. Li, Y. Yuan, "Shaking table test of a multi-story subway station under pulse-like ground motions", *Soil Dynamics and Earthquake Engineering*, Vol. 82, pp. 111-122, 2016.

[10] D. Z. Quan, Y. H. Wang, D. Ye, Y. L. Jing, S Chen, "*Shaking table test study on subway station built in loess area*", *China Civil Engineering Journal*, Vol. 49, no 11, pp. 79-90, 2016. (in Chinese)

[11] D. Z. Quan, "Seismic Response Characteristic and Calculation Method of metro station in Loess", Xi'an, 2016, Chang'an University. (in Chinese)

[12] G. J. Parra-Montesinos, A. Bobet, J. A. Ramirez, "Evaluation of soil-structure interaction and structural collapse in Daikai subway station during Kobe earthquake", *ACI Structural Journal*, Vol. 103, no 1, pp. 113-122, 2006.

[13] X. L. Du, C. Ma, D. C. Lu, C. S. Xu, Z. G. Xu, "Collapse simulation and failure mechanism analysis of the Daikai subway station under seismic loads", *China Civil Engineering Journal*, Vol. 50, no 1, pp. 53-62, 2017. (in Chinese)

[14] T. Liu, Z. Y. Chen, Y. Yuan, X. Y. Shao, "Fragility analysis of a metro station structure by incremental dynamic analysis", *Advances in Structural Engineering*, Vol. 20, no 7, pp. 1111-1124, 2017.

[15] H. B. Liu, E. Song, "Seismic response of large underground structures in liquefiable soils subjected to horizontal and vertical earthquake excitations", *Computers and Geotechnics*, Vol. 32, no 4, pp. 223-244, 2005.

[16] X. H. Bao, Z. F. Xia, G. L. Ye, Y. B. Fu, D. Su, "Numerical analysis on the seismic behavior of a large metro subway tunnel in liquefiable ground", *Tunnelling and Underground Space Technology*, Vol. 66, pp. 91-106, 2017.

[17] C. J. Wang, "Seismic racking of a dual-wall metro station box embedded in soft soil strata", *Tunnelling and Underground Space Technology*, Vol. 26, no 1, pp. 83-91, 2011.

[18] H. Y. Zhuang, G. X. Chen, Z. H. Hu, C. Z. Qi, "Influence of soil liquefaction on the seismic response of a subway station in model tests", *Bulletin of Engineering Geology and the Environment*, Vol. 75, no 3, pp. 1169-1182, 2016.

[19] X. Y. Li, X. G. Jin, Y. S. Feng, W. Luo, "Effect of soft layer on seismic response of subway station in layered stratum", *Journal of Vibroengineering*, Vol. 18, no 3, pp. 1602-1616, 2016.

[20] G. X. Chen, S. Shen, C. Z. Qi, X. L. Du, Z. H. Wang, W. Y. Chen, "Shaking table tests on a three-arch type metro station structure in a liquefiable soil", *Bulletin of Earthquake Engineering*, Vol. 13, no 6, pp. 1675-1701, 2015.

[21] G. X. Chen, S. Chen, X. Zuo, X. L. Du, C. Z. Qi, Z. H. Wang, "Shaking-table tests and numerical simulations on a subway structure in soft soil", *Soil Dynamics and Earthquake Engineering*, Vol. 76, pp. 13-28, 2015.

[22] M. R. Moghadam, M. H. Baziar, "Seismic ground motion amplification pattern induced by a subway tunnel: Shaking table testing and numerical simulation", *Soil Dynamics and Earthquake Engineering*, Vol. 83, pp. 81-97, 2016.

[23] W. Li, W. Zhu, “A dynamic simulation model of passenger flow distribution on schedule-based rail transit networks with train delays”, *Journal of Traffic and Transportation Engineering (English Edition)*, Vol. 3, no 4, pp. 364-373, 2015.

[24] W. H. Zhou, H. Y. Qin, J. L. Qiu, H. B. Fan, J. X. Lai, K. Wang, L. X. Wang, “Building information modelling review with potential applications in tunnel engineering of China”, *Royal Society Open Science*, 2017, doi: 10.1098/rsos.170174.

[25] A. J. Deeks, M. F. Randolph,“Axisymmetric time domain transmitting boundaries”,*Journal of Engineering Mechanics*, Vol. 120, no 8, pp. 25-42, 1994.

[26] J. X. Lai, F. Y. Niu, K. Wang, J. X. Chen, Q. L. Qiu, H. B. Fao, Z. N. Hu,“Dynamic effect of metro-induced vibration on the rammed earth base of the Bell Tower”,*Springplus*,Vol. 2016, Article ID 935,doi: 10.1186/s40064-016-2627-1.

[27] Z. Y. Chen, C. Shi, T. B. Li, Y. Yuan,“Damage characteristics and influence factors of mountain tunnels under strong earthquakes”,*Natural Hazards*, Vol. 61, no 2, pp. 387-401, 2012.

[28] Z. Y. Chen, J. S. Wei,“Correlation between ground motion parameters and lining damage indices for mountain tunnels”,*Natural Hazards*, Vol. 65, no 3, pp. 1683-1702, 2013.

[29] Z. Y. Chen, H. T. Yu, Y. Yuan,“Full 3D seismic analysis of a long-distance water conveyance tunnel”,*Structure and Infrastructure Engineering*, Vol. 10, no 1, pp. 128-140, 2014.

[30] J. X.Lai, H. B. Fan, J. X. Chen, J. L. Qiu, K. Wang,“Blasting vibration monitoring of undercrossing railway tunnel using wireless sensor network”,*InternationalJournal of Distributed Sensor Networks*,Vol. 2015, Article ID 703980, doi: 10.1155/2015/703980.

[31] Z. F. Wang, S. L. Shen, C. Ho, Y. H. Kim,“Investigation of Field Installation Effects of Horizontal Twin-Jet Grouting in Shanghai Soft Soil Deposits”,*Canadian Geotechnical Journal*, Vol. 50, no 3, pp. 288-297, 2013.

[32] Z. F. Wang, S. L. Shen, Z. Y. Yin, Y. S. Xu,“Rapid field evaluation of the strength of cement-stabilized clayey soil”, *Bulletin of Engineering Geology and the Environment*, Vol. 74, no 3, pp. 991-999, 2015.

[33] J. Matsui, K. Ohtomo, K. Kanaya, “Development and Validation of Nonlinear Dynamic Analysis in Seismic Performance Verification of Underground RC Structures”, *Journal of Advanced Concrete Technology*, Vol. 2, no 1, pp. 25-35, 2004.

[34] X. J. Cheng, L. P. Jing, J. Cui, Y. Q. Li, RDong, “Shaking-Table Tests for Immersed Tunnels at Different Sites”,*Shock and Vibration*,Vol. 2017, Article ID 2546318, doi: 10.1155/2017/2546318.